DMD Fast Forward. Published on December 19, 2011 as doi: 10.1124/dmd.111.043562
This article has not been copyedited and formatted. The final version may differ from this version.

DMD #43562

Investigation of figopitant and its metabolites in rat tissue by combining whole body autoradiography with liquid extraction surface analysis mass spectrometry

Simone Schadt, Susanne Kallbach, Reinaldo Almeida, Jan Sandel

Boehringer Ingelheim Pharma GmbH & Co. KG, Biberach, Germany (S.S., S.K., J.S.)

F. Hoffmann-La Roche Ltd, Basel, Switzerland (current address of S.S.)

University of Southern Denmark, Odense, Denmark (R.A.)

Advion Biosciences Ltd, Harlow, UK (R.A.)

Running Title: Distribution of figopitant and its metabolites in rat tissue

Correspondence: Jan Sandel, Boehringer Ingelheim Pharma GmbH & Co KG, Birkendorfer Strasse 65, 88400 Biberach an der Riss, Germany

Telephone: (+49) 7351 54 96897

Fax: **(**+49) 7351 54 90735

E-mail: jan.sandel@boehringer-ingelheim.com

Text Pages: 14

Tables: 3

Figures: 2

References: 16

Abstract: 163

Introduction: 439

Discussion: 634

Abbreviations used in text:

acetonitrile (ACN), below limit of quantification (BLQ), direct analyses in real time (DART), desorption electrospray ionization (DESI), electrospray ionization (ESI), formic acid (FA), full width at half maximum (FWHM), high performance liquid chromatography (HPLC), liquid chromatography (LC), laser desorption ionization (LDI), liquid extraction surface analysis (LESA), liquid scintillation counting (LSC), matrix assisted laser desorption ionization (MALDI), mass spectrometry (MS), tandem mass spectrometry (MS/MS), mass-to-charge ratio (m/z), nanoelectrospray (NSI), parts per million (ppm), quantitative whole-body autoradiography (QWBA), radiochromatogram (RC), single ion monitoring (SIM), solid phase extraction (SPE)

Abstract

This contribution describes the combination of whole body autoradiography with liquid extraction surface analysis (LESA) and mass spectrometry (MS) to study the distribution of the tachykinin NK_1 antagonist figopitant and its metabolites in tissue sections of rats after intravenous administration of 5.0 mg/kg figopitant. An overview of autoradiography results is presented together with mass spectrometry identification and semi-quantification of parent drug and its metabolites based on LESA-MS. The quality and accuracy of data generated by LESA-MS was assessed by comparison to classical tissue extraction, sample cleanup and HPLC analysis. The parent drug and the *N*-dealkylated metabolite M474(1) (BIIF 1148) in varying ratios were the predominant compounds in all tissues investigated. In addition, several metabolites formed by oxygenation, dealkylation, and a combination of oxygenation and dealkylation were identified. In summary, the LESA-MS technique was shown to be a powerful tool for identification and semi-quantification of figopitant and its metabolites in different tissues and was complementary to quantitative whole-body autoradiography (QWBA) for studying the distribution.

Introduction

Quantitative whole-body autoradiography (QWBA) is the imaging method of choice for investigating the distribution of drug-related radioactivity in all organs and tissues of an intact organism such as an animal carcass. With this technique, information on the concentration of the entire drug-related radioactivity is gained. However, the actual molecular entity - parent compound or metabolites - and their respective proportions of the radioactivity remains unknown. The conventional approach to identify and quantify parent drug and metabolites in tissues is the preparation of organ homogenates and sample analysis by liquid chromatography combined with radiodetection and tandem mass spectrometry. However, this approach is labour-intensive, and some tissues (e.g. salivary glands) and tissue substructures (e.g. renal inner and outer medulla) can be difficult or even impossible to sample and extract. Surface sampling methods such as desorption electrospray ionization (DESI), laser desorption ionization (LDI), direct analyses in real time (DART), or matrix assisted laser desorption ionization (MALDI) can speed up analysis time and cut overall costs compared to classical tissue extraction and enable spacial resolution of different anatomical substructures within a given organ (Reyzer et al., 2003).

Recently, a fully automated liquid extraction based surface sampling method for mass spectrometry analyses of drugs and metabolites in thin tissue sections has been described (Van Berkel and Kertesz, 2009; Kertesz and Van Berkel, 2010). This LESA method uses a liquid micro junction probe to extract the analytes directly from the surface followed by automated nanoelectrospray analysis. Direct surface sampling methods deal with high sample complexity, since no chromatographic separation is involved. To maintain the high dynamic range and mass accuracy across the whole mass range, an optimized strategy can be used by collecting multiple adjacent SIM windows (Southam and Viant, 2007), if a continuous long and stable analyte signal

is obtained. For LESA-MS, the typical volume used for the microextraction of 1-2 µL enables the long analyte signal (~20 min) needed for the SIM strategy, which cannot be accomplished by the other surface sampling methods.

This contribution describes the investigation of tissue sections of rats after intravenous administration of 5.0 mg/kg [14C]figopitant, a tachykinin NK_1 antagonist (Ohmura et al., 2004). The approach applied here involved no additional sample preparation step. Tissue sections prepared for QWBA were used directly for LESA-MS in a fast and robust method. An overview of autoradiography results is presented together with the corresponding results of LESA-MS. The quality and accuracy of data generated by LESA-MS is assessed by comparison to classical tissue extraction, sample cleanup and HPLC analysis. For a variety of different tissues, this comparison was performed using two different animals, whereas for liver, the same animal was used.

Methods

Materials

Figopitant hydrochloride (BIIF 1149 CL, ((S)-N-[2-[3,5-bis(trifluoromethyl)phenyl]ethyl]-4-(cyclopropylmethyl)-N-methyl-α-phenyl-1-piperazineacetamide, monohydrochloride, monohydrate)) is a neurokinin-1 receptor antagonist (Ohmura et al., 2004). Figopitant hydrochloride (batch no. RAL 105) and the synthetic reference compounds BIIF 1148 CL2 ((S)-N-[2-[3,5-bis(trifluoromethyl)phenyl]ethyl]-N-methyl-α-phenyl-1-piperazineacetamide, dihydrochloride)) and BIIF 1276 (mixture of diastereoisomeres) were synthesized at Boehringer Ingelheim GmbH & Co KG, Germany. Radio-labeled [14C]figopitant hydrochloride (batch no. Ks 447/23) was obtained from the isotope chemistry laboratory of Boehringer Ingelheim, Germany, and had a radiochemical purity (as determined by HPLC) greater than 97.0%.

High performance liquid chromatography (HPLC) grade acetonitrile (ACN) and methanol (MeOH) were purchased from Merck (Darmstadt, Germany). Formic acid (FA) (p.a. ~ 98% purity) was purchased from Sigma Aldrich (Schnelldorf, Germany). Water was demineralized and purified by distillation in house.

Study conduct

Dose formulation

The formulation was prepared on the day of dosing. The target dose was 5.0 mg/kg [14C]figopitant free base which corresponds to 5.52 mg/kg [14C]figopitant hydrochloride. 5.034 mg of radio-labeled substance was dissolved in 2.055 mL of phosphate buffer with a pH of 6.0. The final concentration of intravenously administered test substance solution was 2.21 mg/mL with a specific activity of 0.3877 MBq/µmol.

Animal experiment

Male albino Wistar Hannover rats (in-house bred strain: Chbb:THOM) with body weights ranging from 165 to 175 g were housed individually in standard macrolon cages under standardized environmental conditions (e.g. 12:12 hours of light:dark cycle). From 20 hrs before test substance administration via oral gavage until sacrifice at 4 hours after dosing, the animals were kept fasted with tap water being available at any time. At 5 min, 4 hrs, 24 hrs and 144 hrs after intravenous administration one rat per time point was anesthetized with halothane. For determination of radioactivity concentrations in whole blood and plasma by liquid scintillation counting (LSC) as well as the packed cell volume (hematocrit), blood samples were withdrawn from the retrobulbar venous plexus immediately prior to sacrifice. While still under general anesthesia, the animals were sacrificed by inhalation of an overdose of chloroform. After

euthanasia, the rat carcasses were deep frozen in a saturated solution of dry ice in ethanol. For verification purpose, two additional male albino Wistar rats (strain: Crl:WI(Han)) were sacrificed at 4 hours (C(max)) after intravenous administration. One carcass was intended for QWBA, the other was dissected. All tissues obtained by dissection were submitted to extraction (cf. Analysis of tissue sections and samples). The *in-vivo* experiment was conducted entirely in accordance with the German animal welfare law (Tierschutzgesetz).

Preparation of tissue sections

Following removal of legs and tail, the frozen carcass was set in a block of aqueous 3% (w/v) carboxymethyl cellulose and mounted onto the stage of a CM 3600 cryomacrocut maintained at -24°C (Leica Microsystems GmbH). For quantitation of radioactivity in tissues, seven calibration standards of human whole blood spiked with a 14C-labeled reference compound in concentrations ranging from 2×10^3 to 2×10^6 dpm/mL were embedded in each block. Sagittal sections with a target thickness of 30 µm were obtained at up to 3 levels through the carcass: (a) ocular bulb/kidney, (b) adrenal gland and (c) pituitary gland/spinal cord (median) at -22°C according to the method of Ullberg (1977). The sections, mounted on transparent tape (No. 4248 Tesafilm, Beiersdorf AG), were freeze-dried for 24 hours in the cryomacrocut. A thin layer of talcum powder was applied to the dehydrated section-bearing tapes in order to avoid adhesion and electrostatic charge effects.

Analysis of tissue sections and samples

Quantitative whole-body autoradiography

The dehydrated and talcumized sections were exposed on FUJI imaging plates (BAS-SR 2025) for 7 days. After exposure, the imaging plates were processed using the Bio-Imaging Analyser

FUJIX BAS 2000 (raytest GmbH). The tissues were anatomically identified by AIDA (raytest GmbH) assisted superposition of electronic whole-body autoradiogram and related scanned section. The concentrations of radioactivity in the identified tissues were quantified using a calibration curve over the (LSC controlled) range of radioactivity concentrations, which was created based on the phosphor stimulated luminescence measured in the image of the embedded [14C]blood standards and their radioactivity concentrations in general accord with the approach described by Schweitzer at al. (1987). The tissue concentration data are expressed in terms of ng equivalent of [14C]figopitant free base per gram tissue [ng-eqv/g]. The lower and upper limits of quantification for the procedure were 32 to 33,625 ng-eqv/g. For the purpose of quantification, it was assumed that all tissues analyzed had density and quench characteristics similar to whole blood (as used for calibration standards). Dependent on organ size, up to 4 subareas per tissue within a single autoradiogram were defined for quantification and statistics (e.g. for the liver 16 subareas from 4 autoradiograms of one animal and time point with a CV of 10.2%).

Extraction of Tissues

The following tissues were homogenized and extracted at 4 hours after intravenous administration of 5 mg/kg [14C]figopitant to rat: liver, kidney, lung, spleen, pancreas, myocardium, muscle, white fat, brown fat, brain, salivary gland, thymus, stomach, testis, Harderian's gland, epididymis, and pituitary. In addition, liver tissue obtained from the same rat that was used for LESA-MS was homogenized and extracted for LC/radiometry/MS analysis. Liver was cut from the remainder of the frozen carcass blocked in aqueous carboxymethyl cellulose after preparation of tissue sections.

Typical sample preparation procedures are described as follows. Tissues were homogenized in water (1 mL/g) using a Potter S homogenizer (B. Braun Biotech International, Germany). Tissue

DMD Fast Forward. Published on December 19, 2011 as DOI: 10.1124/dmd.111.043562
This article has not been copyedited and formatted. The final version may differ from this version.

homogenates were processed by extensive extraction with 10 mL 0.1 % formic acid in 70 % aqueous ACN, 0.1 % formic acid in 80 % aqueous ACN, and 0.1 % formic acid in 100 % ACN. Recoveries of each extraction step were monitored by LSC measurement and extractions were continued until > 95 % of total radioactivity were extracted. The samples were shaken for 3 min with a mechanical shaker and ultrasonicated extensively, then centrifuged for 10 min at 4000 rpm. The extracts were combined and concentrated by lyophilization. For SPE, cartridges were preconditioned with ACN and equilibrated with water containing 0.1 % formic acid. After applying the tissue extracts onto the column and rinsing with 0.1 % formic acid in water, the adsorbed material was eluted with 0.1 % formic acid in 80 % aqueous ACN and 0.1 % formic acid in 100 % ACN. The combined eluates were concentrated by lyophilization.

The samples were analyzed by nanoelectrospray ionization mass spectrometry (LC-NSI-MS) in the positive ion mode using a linear ion trap/Orbitrap hybrid mass spectrometer (Thermo Scientific, Germany) (Hu et al., 2005) equipped with a Triversa Nanomate^{TM} nanospray ion source (Advion BioSciences, USA) (Schultz et al., 2000, Ramanathan et al., 2007). The instrument was coupled to a Berthold LB 509 (Berthold Technologies, Germany) radioactivity detection system.

LC separation of the metabolites was performed by an optimized method: A YMC Triart column (YMC Europe GmbH, Germany) with the dimension 150 × 4.6 mm, particle size 3 µm with a YMC ODS-AQ guard column (10 × 4 mm, particle size 5 µm) at a flow rate of 1000 µL/min was used. The injection volume was set to 10 - 500 µL, and the column oven temperature was 40°C. The mobile phase consisted of 10 mM ammonium formate solution acidified with 0.1% formic acid (mobile phase A) and acetonitrile with 0.1 % formic acid (mobile phase B). The following gradient was applied: 0.0 to 3.0 min linear from 5 % to 35 % B, 3.0 to 35.0 min linear from 35 % to 50 % B, 35.0 to 40.0 min linear from 50 % to 95 % B, 40.0 to 45.0 min isocratic 95 % B and

45.1 to 50 min reequilibration at 5 % B. For the LC-NSI-MS experiments, the LC flow (1.0 mL/min) was split post column with about 170 µL/min going to the Triversa Nanomate™ and the remaining to the on-line radioactivity detector. After an additional splitter within the Triversa Nanomate™, about 600 nL/min went into the NSI source. The Triversa Nanomate™ software was operated in spray sensing mode to automatically change to the nozzle for two consecutive times in case of clogging. The Orbitrap mass analyzer was operated at a resolution of approximately 60,000 FWHM at m/z 400 in the full scan MS mode. High-resolution mass spectra were acquired in the range of m/z 100 to 1200. Accurate mass measurement was performed after external calibration using the manufacturer's calibration mixture prior LC-MS investigations.

Sample Analysis by LESA-MS

Samples obtained from the freeze-dryed 30 µm whole body sections were analyzed using a linear ion trap LTQ/Orbitrap hybrid mass spectrometer (Thermo Scientific, Germany) (Hu et al., 2005) equipped with a TriVersa Nanomate™ nanospray ion source (Advion BioSciences, USA) (Schultz et al., 2000, Ramanathan et al., 2007). For sample extraction from the tissue sections, 1-2 µL of solvent (ACN/water 50:50 with 0.1% formic acid) were used. Solvent was dispensed on the tissue sample and aspirated again after 2 sec. This step was repeated 3 times. The spot that was extracted had a diameter of approximately 1 mm. The infusion rate was approximately 50 - 100 nL/min. Two separate MS methods were designed for metabolite identification and metabolite quantification. For metabolite identification, a method with 400 scan events alternating between MS and MS^2 experiments in 5 Da steps with an overlap of 2.5 Da in the range of m/z 250 to 750 was designed. For metabolite quantification, a single ion monitoring (SIM) scan method with a mass window of the accurate mass of the metabolites +/- 2.5 Da was applied. The relative abundance of metabolites was assessed based on average MS peak intensity

with a mass tolerance of 5 ppm. Concentrations of metabolites at the sample spots were calculated based on total radioactivity within these spots which were obtained from QWBA.

Data Analysis

The relative concentration of individual metabolites as percent of total drug related material was calculated as follows:

$c(M_i)$ (% of total drug related material) = $A(M_i) / \Sigma_i A(M_i) * 100$

$c(M_i)$: relative concentration of individual metabolite

$A(M_i)$: peak area of individual metabolite

$\Sigma_i A(M_i)$: sum of peak areas of all metabolites and parent detected within the LESA run

The absolute amounts of individual metabolites in ng/kg was calculated based on the relative percentage of metabolites and the absolute amount of radioactive compound as determined by autoradiography.

Results

Autoradiography results

After intravenous administration of 5.0 mg/kg [14C]figopitant, the total drug-related radioactivity was quickly (judged on the first time point at 5 minutes post dosing) and extensively distributed into all tissues of the body including significant levels in the central nervous system. At 4 hrs after intravenous administration, maximum concentrations (Cmax) of total drug-related radioactivity were reached in liver, spleen, thymus, testis, epididymis, Harderian gland, skin and adipose tissue (Figure 1). Due to biliary excretion and presumably also gastro-intestinal secretion the highest amounts of radioactivity at 4 hours post dosing were found in the gastro-intestinal

contents (chyme). Except for the situation in testis with a very long half-life of about 4 days, total drug-related radioactivity was cleared from all other tissues with half-lives of about 20 to 40 hrs (Table 1).

Extraction of Tissues

Tissue extractions were considered to be essentially complete, as more than 96.9 % of total sample radioactivity was extracted for all tissues. SPE recoveries were in the range of 90 – 110 % of sample radioactivity. Metabolite patterns were assessed using HPLC coupled to online radioactivity detection and metabolites were identified by liquid chromatography mass spectrometry (LC-MS/MS) measurements. Chemical structures were elucidated by LC-MS/MS and by comparison to synthetic reference compounds if available. The parent drug and the *N*-dealkylated metabolite M474(1) (BIIF 1148) in varying ratios were the predominant compounds in all tissues. In addition, several metabolites formed by oxygenation (M544(1), M544(2) (BIIF 1276), and M544(3), oxygenation and dehydrogenation (M542(1), dealkylation (M448(1)), and a combination of oxygenation, dehydrogenation and dealkylation (M488(1), M490(1)) were found. A synopsis of figopitant metabolites in rat tissue is presented in figure 2, and corresponding LC-MS data is depicted in table 2. The relative abundance of metabolites (% of total radioactivity) in different tissues is presented in table 3.

Sample Analysis by LESA-MS

Thin tissue sections from a rat administered intravenously with figopitant were analyzed and compared to extracted tissues of another rat. In addition, after obtaining tissue sections, the remainder of the liver was cut from the CMC block for LC/radiometry/MS. Metabolite identification in tissue sections was performed using MS optimized for maximum sensitivity and

MS/MS to facilitate the search for metabolites. For semiquantification of metabolites, a SIM scan method (+/- 2.5 Da) for the eight metabolites identified with the survey method (Table 2) was applied. The signal levels of the SIM scans were consistent over the analysis time of 5 min. The relative abundance of metabolites was assessed based on extracted ion chromatograms with a mass tolerance of 5 ppm (Table 3). For each tissue, three different spots were analyzed by LESA-MS. The same spot could be analyzed at least 18 times, yielding the same metabolic pattern, however the intensity of the MS signal dropped. There was no major difference in metabolic pattern of tissues when different solvent compositions (5 % aqueous ACN, 50 % aqueous ACN) were used for extraction, however, the signal intensity was higher with 50 % ACN compared to 5 % ACN.

LESA-MS of tissue sections showed that the drug substance and the *N*-dealkylated metabolite M474(1) (BIIF 1148) were the predominant compound in all tissues. There was no qualitative difference between LESA analysis and HPLC analysis of extracted tissues, and all major metabolites identified in tissue extracts were also found with LESA. However, isobaric metabolites like M544(1), M544(2), and M544(3) cannot be distinguished by LESA-MS because there is no chromatographic separation. The relative abundance of metabolites (% of drug related compounds) in different tissues quantified using LESA is presented and compared to radioactive quantification data in table 3.

In addition, liver tissue obtained from the same rat that was used for tissue sections was homogenized, extracted and analyzed by LC/radiometry/MS and compared to results obtained by LESA. The relative abundance of metabolites (% of drug related compounds) and absolute metabolite concentrations are listed in Table 4.

Discussion

Following intravenous administration of figopitant to rats, the parent drug and the *N*-dealkylated metabolite M474(1) in varying ratios were predominant in all tissues investigated. In addition, several metabolites formed by oxygenation, dealkylation, and a combination of oxygenation and dealkylation were identified. Extraction of tissues followed by radiochromatographic analysis yielded the same qualitative and comparable quantitative results as LESA-based analysis of tissue sections. The experimental approach applied here involved no sample preparation steps. Tissue sections prepared for autoradiography were used directly for LESA-MS.

Analysis of the liver of the same animal by extraction and radiochromatography compared to LESA-based quantification are in good agreement. The most prevalent compounds (M474(1), M490(1) and Figopitant) could be quantified by LESA-MS with accuracies between 82 and 110 %. For low abundant metabolites, integration of chromatographic peaks is less accurate compared to higher abundant metabolites. Therefore, LESA-MS-based and radiometric quantification deviate more for lower abundant metabolites. As there is no chromatographic separation, the isobaric metabolites M544(1), M544(2), and M544(3) cannot be distinguished by this methodology. M544(1), M544(2), and M544(3) are low abundant metabolites, therefore the radiometric quantification becomes less accurate, especially if one or two isomers are below the limit of radiometric quantification (500 dpm on column).

For all other organ analysis, different animals were used for LESA-MS-based and radiometric quantification, and therefore, the interindividual variability has to be considered as well. The extent of the interindividual variability can be seen when comparing the radiometric quantification of the liver extract of the two different animals (Table 3 and Table 4). For both animals, M474(1) was the major metabolite (61.4 % and 53.6 % of total), followed by M490(1), accounting for 16.2 % and 19.5 %, respectively. The parent drug accounted for 11.7 % and 9.3 %.

Metabolite M488(1) was apparently not present in significant amounts in the animal used for LESA, but in the animal used for tissue extraction and radiometric quantification. In addition to the interindividual variability, there can be also variability in respect to distribution of parent drug and metabolites within certain organs and organ substructures, for example in different regions of the brain. This has to be kept in mind when homogenates that are an average over the whole tissue are compared to the localized areas samples by LESA-MS. Furthermore, this probably also contributes to higher CV values for LESA-MS of metabolites in certain tissues.

In addition to these animal experimental limitations, MS-based quantification without reference standards can only be considered to be semi-quantitative. MS response can vary significantly depending on the analyte ionization efficiency, sample matrix, LC mobile phase, etc. (Hop et al., 2005). Differences in ionization efficiency of compounds with different physico-chemical characteristics are in general reduced by the application of chip-based nanoelectrospray (NSI) (Hop et al., 2005; Hop et al., 2006; Wickremsinhe et al., 2006; Valaskovic et al., 2006; Ramanathan et al., 2007). Recently, the accuracy of nanoelectrospray ionization MS response of drug compounds and their respective metabolites from biological matrices compared to accurate radiometric quantification was evaluated, and it has been demonstrated that nanoelectrospray mass spectrometry can be used for semi-quantitation of metabolites (Schadt et al., 2011). For LESA-MS, the accuracy of semi-quantification results was expected to be even higher, as no chromatographic separation was used, and therefore, different LC mobile phase compositions and matrix effects could not contribute to variations in MS response.

In conclusion, the LESA technique was found to be a powerful tool for identification and and semi-quantitation of figopitant and its metabolites in tissue sections. Figopitant and its *N*-dealkylated metabolite M474(1) (BIIF 1148) in varying ratios were the predominant compounds in all tissues. In this study, LESA-MS provided results that are complementary to

QWBA. By LESA-MS, major metabolites in a variety of different tissues can be identified and relative quantitation of metabolites are achieved by MS. Furthermore, combination LESA with QWBA provide semiquantitation of absolute metabolite levels in tissue.

Acknowledgements

The authors would like to thank the following colleagues from Boehringer Ingelheim Pharma GmbH & Co. KG (Biberach, Germany): Jürgen Baierl and Oxana Gerling for their excellent technical assistance, Ralf Kiesling for providing the radio-labeled figopitant hydrochloride, Dr. Rudolf Binder, Dr. Dirk Trommeshauser and Dr. Lin-Zhi Chen for their revision of the manuscript, and Dr. Thomas Ebner, Dr. Andreas Greischel and Dr. Ulrich Roth for their support of the project.

Authorship Contributions

Participated in research design: Schadt, Almeida, Sandel

Conducted experiments: Almeida, Kallbach

Performed data analysis: Schadt, Kallbach Almeida, Sandel

Wrote or contributed to the writing of the manuscript: Schadt, Almeida, Sandel

References

Hop CECA, Chen Y, Yu LJ (2005) Uniformity of ionization response of structurally diverse analytes using a chip-based nanoelectrospray ionization source. *Rapid Commun Mass Spectrom* **19**: 3139-3142.

Hop CECA (2006) Use of nano-electrospray for metabolite identification and quantitative absorption, distribution, metabolism and excretion wtudies. *Curr Drug Metab* **7**: 557-563.

Hu Q, Noll RJ, Li H, Makarov A, Hardman M, Cooks RG (2005) The Orbitrap: a new mass spectrometer. *J Mass Spectrom* **40**: 430-443.

Kertesz V, Van Berkel GJ (2010) Fully automated liquid extraction-based surface sampling and ionization using a chip-based robotic nanoelectrospray platform. *J Mass Spectrom* **45**: 252-260.

Ohmura T, Hayashi T, Satoh Y, Konomi A, Jung B, Satoh H (2004) Involvement of substance P in scratchig behaviour in a atopic dermatitis model. *Eur J Pharmacol* **491**: 191-194.

Ramanathan R, Zhong R, Blumenkrantz N, Chowdhury SK, Alton KB (2007) Response normalized liquid chromatography nanospray ionization mass spectrometry. *J Am Soc Mass Spectrom* **18**: 1891-1899.

Reyzer ML, Hsieh Y, Ng K, Korfmacher WA, Caprioli RM (2003) Direct analysis of drug candidates in tissue by matrix-assisted laser desorption/ionization mass spectrometry. *J Mass Spectrom* **38**: 1081-1092.

Schadt S, Chen LZ, Bischoff D (2011) Evaluation of relative LC-MS response of metabolites to parent drug in LC/Nanospray ionization mass spectrometry: Potential implications in MIST assessment. *J Mass Spectrom* **46**: 1281-1286.

Schultz GA, Corso TN, Prosser SJ, Zhang S (2000) A fully integrated monolithic microchip electrospray device for mass spectrometry. *Anal Chem* **72**: 4058-4063.

Schweitzer A, Fahr A, Niederberger W. (1987) A simple method for the quantification of 14C-whole-body autoradiograms. *Appl Radiat Isot* **38**: 329-333.

Southam AD, Payne TG, Cooper HJ, Arvanitis TN, Viant MR (2007) Dynamic range and mass accuracy of wide-scan direct infusion nanoelectrospray fourier transform ion cyclotron resonance mass spectrometry-based metabolomics increased by the spectral stitching method. *Anal Chem* **79**: 4595-4602.

Tierschutzgesetz: http://www.gesetze-im-internet.de/tierschg/index.html

Ullberg S (1977) The technique of whole-body autoradiography. Cryosectioning of large specimens. In: Special Issue on Whole-Body Autoradiography. Science Tools, The LKB Instrument Journal **1**: 2-29.

Valaskovic GA, Utley L, Lee MS, Wu JT (2006) Ultra-low flow nanospray for the normalization of conventional liquid chromatography/mass spectrometry through equimolar response: standard-free quantitative estimation of metabolite levels in drug discovery. *Rapid Commun Mass Spectrom* **20**: 1087-1096.

Van Berkel GJ, Kertesz V (2009) Application of a liquid extraction based sealing surface sampling probe for mass spectrometric analysis of dried blood spots and mouse whole-body thin tissue sections. *Anal Chem* **81**: 9146-9152.

Wickremsinhe ER, Singh G, Ackermann BL, Gillespie TA, Chaudhary AK (2006) A review of nanoelectrospray ionization applications for drug metabolism and pharmacokinetics. *Curr Drug Metab* **7**: 913-928.

Figure legend

Figure 1: Autoradiogram of a male albino rat at 4 hours after intravenous administration of 5.0 mg/kg [14C]figopitant (sagittal section at ocular bulb-kidney-level)

Figure 2: Metabolism pathways of figopitant (rectangle) in rats after intravenous infusion of 5.0 mg/kg of [14C]figopitant to male albino rat. Structures of metabolites were characterized by mass spectrometry.

Tables

Table 1 Concentrations and half-lives of total drug-related radioactivity in tissues of male albino rats after intravenous administration of 5.0 mg/kg [14C]figopitant

Organ system Tissue	*5 min* *[ng-eqv/g]*	**4 hrs** **[ng-eqv/g]**	*24 hrs* *[ng-eqv/g]*	*t½* *[h]*
locomotor apparatus				
muscle cranial	*8,437*	**2,972**	*671*	*ND*
muscle caudal	*6,936*	**2,606**	*670*	*19.7*
digestive apparatus				
tongue	*12,885*	**3,786**	*891*	*ND*
salivary gland	*10,729*	**8,238**	*1,877*	*20.3*
liver	*5,984*	**13,851**	*4,793*	*31.2*
pancreas	*17,869*	**12,820**	*4,138*	*ND*
adipose tissue	*467*	**537**	*113*	*27.1*
respiratory apparatus				
lung	*24,769*	**10,036**	*1,708*	*20.5*
urogenital apparatus				
renal cortex	*19,088*	**8,020**	*2,627*	*ND*
testis	*938*	**1,510**	*633*	*95.6*
epididymis	*1,728*	**2,290**	*1,043*	*ND*
endocrine glands				
adrenal cortex	*21,006*	**11,078**	*3,447*	*ND*
pituitary	*8,110*	**7,747**	*2,350*	*ND*

cardiovascular system				
myocardium	*13,504*	**4,240**	*1,207*	*ND*
spleen	*7,308*	**10,694**	*3,306*	*ND*
thymus	*3,243*	**3,372**	*1,746*	*22.7*
bone marrow	*4,445*	**3,910**	*1,156*	*ND*
whole blood (LSC)	*830*	**361**	*122*	*38.6*
plasma (LSC)	*483*	**192**	*80*	*21.9*
central nervous system				
brain (total)	*1,912*	**122**	*50*	*32.7*
sense organ (eye)				
Harderian gland	*4,132*	**13,941**	*6,246*	*ND*
common integument				
skin (total)	*1,743*	**1,997**	*606*	*ND*

ND = not determined

DMD Fast Forward. Published on December 19, 2011 as DOI: 10.1124/dmd.111.043562
This article has not been copyedited and formatted. The final version may differ from this version.

Table 2: LC-MS data of figopitant and metabolites (Compounds are listed in order of nominal $[M+H]^+$ masses.

Metabolite Code	**Synthetic Reference Compound**	**Retention Time**, min	**$[M+H]^+$** m/z, Th (Δm, ppm)	**Product Ions** m/z, Th (Δm, ppm)
M448(1)		11.9	$C_{21}H_{24}ON_3F_6$ 448.18181 (0.31)	431.15526 (-0.60), 360.11815 (3.95), 149.10732 (-0.68)
M474(1)	**BIIF 1148**	14.5	$C_{23}H_{26}ON_3F_6$ 474.19746 (-0.99)	360.11815 (0.73), 175.12298 (-1.60)
M488(1)		13.4	$C_{23}H_{24}O_2N_3F_6$ 488.17672 (-0.50)	175.12298 (-0.46)
M490(1)		12.7	$C_{23}H_{26}O_2N_3F_6$ 490.19237 (-0.10)	175.12298 (-0.11)
M542(1)		18.3	$C_{27}H_{30}O_2N_3F_6$ 544.22367 (0.60)	229.16993 (1.78)
M544(1)		16.1	$C_{27}H_{32}O_2N_3F_6$ 544.23932 (-0.34)	229.16993 (1.12)
M544(2)	**BIIF 1276**	24.2	$C_{27}H_{32}O_2N_3F_6$ 544.23932 (-0.79)	360.11815 (3.78), 229.16993 (0.85), 138.11515 (-2.81)
M544(3)		14.7	$C_{27}H_{32}O_2N_3F_6$ 544.23932 (-0.57)	229.16993 (7.9)
M528(1)	**BIIF 1149**	21.5	$C_{27}H_{32}ON_3F_6$ 528.24441 (-1.44)	360.11815 (1.75), 229.16993 (1.05), 139.12298 (1.90)

DMD Fast Forward. Published on December 19, 2011 as DOI: 10.1124/dmd.111.043562
This article has not been copyedited and formatted. The final version may differ from this version.

Table 3: Comparison of radioactivity-based quantification and LESA quantification of figopitant and its metabolites in different tissues of two different animals.

Tissue	Metabolite	relative abundance, %					LESA CV, %	LESA Accuracy, %	LESA, nmol/kg
		Organ Extraction	LESA1	LESA2	LESA3	LESA mean			
lung	M474	42.2	57.9	51.6	40.5	50.0	18	118	13242
	M490	3.2	3.2	2.7	2.1	2.7	21	83	706
	Figopitant	48.6	32.1	37.2	47.4	38.9	20	80	10302
	M542	1.0	BLQ	1.3	1.6	1.5	15	145	384
	M544	5.0	6.8	7.2	8.4	7.5	11	149	1977
spleen	M474	42.8	54.7	58.4	60.5	57.9	5	135	22196
	M490	7.5	5.5	5.6	5.5	5.5	1	74	2122
	Figopitant	45.2	33.7	31.1	27.8	30.9	10	68	11840
	M544	4.5	6.1	4.9	6.2	5.7	13	127	2199
kidney (o. m.)	M474	59.2	69.9	71.5	69.2	70.2	2	119	18250
	M490	9.7	8.3	9.1	9.8	9.1	8	93	2357
	Figopitant	31.1	21.9	19.4	21	20.8	6	67	5399
salivary gland	M474	24.1	50.7	47.7	45.2	47.9	6	199	12949
	M488	3.2	1.5	1.2	1.1	1.3	16	40	461
	M490	3.2	4.2	3.6	3.2	3.7	14	115	1413
	Figopitant	67.5	39.2	42.4	45.8	42.5	8	63	11718
	M544	2.0	4.4	5.1	4.8	4.8	7	238	2307
white fat	M474	10.9	BLQ	BLQ	BLQ	NA	NA	NA	NA
	Figopitant	89.1	100.0	100.0	100.0	100.0	NA	112	1257
myo-cardium	M474	66.0	77.0	76.7	78.5	77.4	1	117	9136
	Figopitant	34.0	23.0	23.3	21.5	22.6	4	66	2668
liver	M448	8.6	3.6	3.4	2.9	3.3	11	38	1006
	M474	53.6	62.1	61.4	63.2	62.2	1	116	18978
	M488	3.5	BLQ	BLQ	0.9	0.9	NA	26	274
	M490	19.5	12.4	11.7	15.6	13.2	16	68	4036
	Figopitant	9.3	14.4	14.7	9.6	12.9	22	139	3934
	M542	1.6	BLQ	BLQ	BLQ	NA	NA	NA	NA
	M544	3.9	7.5	8.8	7.9	8.1	8	207	2460
pancreas	M448	2.4	BLQ	BLQ	1.4	1.4	NA	58	437
	M474	40.6	56.5	58.1	53.0	55.9	5	138	17437
	M488	4.9	BLQ	0.5	1.5	1.0	71	20	312
	M490	9.1	7.6	9.3	6.7	7.9	17	86	2455
	Figopitant	29.7	22.8	20.7	27.7	23.7	15	80	7407
	M542	3.5	BLQ	BLQ	BLQ	NA	NA	NA	NA

DMD Fast Forward. Published on December 19, 2011 as DOI: 10.1124/dmd.111.043562
This article has not been copyedited and formatted. The final version may differ from this version.

	M544	9.7	13.1	11.4	9.7	11.4	15	118	3561
thymus	M474	20.9	17.9	27.3	23.3	22.8	21	109	2785
	Figopitant	72.2	69.7	63.1	68.7	67.2	5	93	8192
	M542	4.4	1.8	0.9	0.9	1.2	43	27	146
	M544	2.5	10.6	8.7	7.1	8.8	20	352	1073
stomach	M474	46.4	44.1	44.7	50.2	46.3	7	100	NA
	M488	5.8	1.9	1.9	2	1.9	3	33	NA
	M490	7.7	7.6	6.3	11.3	8.4	31	109	NA
	Figopitant	32.6	39.6	35.6	28.7	34.6	16	106	NA
	M542	4.7	0.6	4.5	BLQ	2.6	108	54	NA
	M544	2.9	6.3	7	7.9	7.1	11	244	NA
testis	M474	7.7	4.4	8.1	7.2	6.6	29	85	131
	Figopitant	72.8	78.9	78.5	81.1	79.5	2	109	1591
	M544	19.6	16.7	13.4	11.7	13.9	18	71	279
Harder´s gland	M474	12.7	16.0	19.8	24.5	20.1	21	158	6884
	Figopitant	87.3	84.0	80.2	75.5	79.9	5	92	27367
epi-didymis	M474	14.4	13.0	28.6	28.3	23.3	38	162	1162
	Figopitant	74.1	70.2	62.5	53.5	62.1	13	84	3095
	M544	11.5	16.7	8.8	18.2	14.6	35	127	726
muscle	M488	4.1	0.9	0.9	0.9	0.9	0	22	62
	M474	38.9	56.9	50.7	59.1	55.6	8	143	3851
	M490	3.7	2.6	0.9	4.1	2.5	63	68	176
	Figopitant	53.7	35.4	44.0	30.2	36.5	19	68	2532
	M542	1.5	BLQ	BLQ	BLQ	NA	NA	NA	NA
	M544	2.1	4.2	3.5	5.6	4.4	24	211	307
pituitary	M448	0.8	0.2	0.2	0.3	0.2	25	29	95
	M474	31.4	44.0	43.3	37.3	41.5	9	132	16974
	M488	2.7	1.1	0.8	0.6	0.8	30	31	341
	M490	4.6	3.5	3.3	3.2	3.3	5	72	1362
	Figopitant	48.8	46.1	46.5	50.8	47.8	5	98	19535
	M542	2.3	0.6	0.2	0.4	0.4	50	17	163
	M544	9.4	4.5	6.0	7.4	6.0	24	63	2439
brain (total)	M474	27.7	11.4	34.3	27.6	24.4	48	88	97
	Figopitant	72.3	88.6	65.7	72.4	75.6	16	105	301
brown fat	M474	60.0	53.7	50.8	54.2	52.9	3	88	7095
	Figopitant	40.0	46.3	49.2	45.8	47.1	4	118	6318

DMD Fast Forward. Published on December 19, 2011 as DOI: 10.1124/dmd.111.043562
This article has not been copyedited and formatted. The final version may differ from this version.

Table 4: Comparison of radioactivity-based quantification and LESA quantification of figopitant and its metabolites in liver of the same animal.

	relative abundance, %		**absolute quantification, nmol/kg**		
Metabolite	**Organ Extraction**	**LESA mean**	**Organ Extraction**	**LESA**	**Accuracy, %**
M448	6.4	3.3	1952	1006	52
M474	61.4	62.2	18724	18978	101
M488	BLQ	0.9	BLQ	274	NA
M490	16.2	13.2	4940	4036	82
Figopitant	11.7	12.9	3568	3934	110
M542	BLQ	BLQ	BLQ	BLQ	NA
M544	4.3	8.1	1311	2460	188

BLQ: below limit of quantification

NA: not applicable

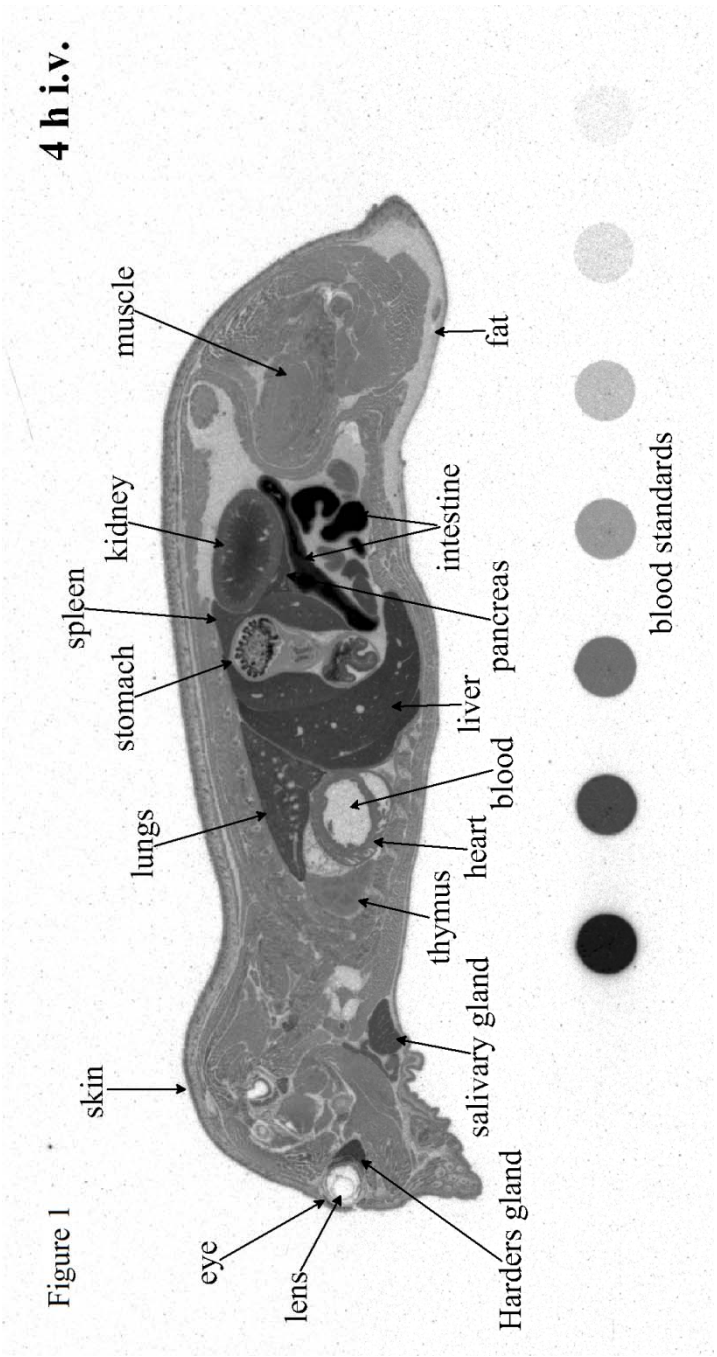

Figure 1

Figure 2